Chinese Chemical Letters 33 (2022) 2692–2696

Contents lists available at ScienceDirect

Chinese Chemical Letters

journal homepage: www.elsevier.com/locate/cclet

Ultrasensitive determination of mercury by ICP-OES coupled with a vapor generation approach based on solution cathode glow discharge

Zhaoqing Cai[a,b], Huijun Zou[a], Yirui Chen[a], Zheng Wang[a,b,*]

[a] Shanghai Institute of Ceramics, Chinese Academy of Sciences, Shanghai 200050, China
[b] Center of Materials Science and Optoelectronics Engineering, University of Chinese Academy of Sciences, Beijing 100049, China

ARTICLE INFO

Article history:
Received 7 July 2021
Revised 25 August 2021
Accepted 14 September 2021
Available online 13 October 2021

Keywords:
Solution cathode glow discharge
Vapor generation
ICP-OES
Mercury
Microplasma

ABSTRACT

We herein proposed a sample introduction technique based on solution cathode glow discharge (SCGD) of a portable design for inductively coupled plasma-optical emission spectrometry (ICP-OES) and its application in sensitive determination of mercury. The products from SCGD containing mercury vapor, were transported by an Ar flow to ICP spectrometer for detection. A gas liquid separator (GLS) and a dryer were used to condense and remove most of the accompanying moisture, which greatly improved both the stability and sensitivity of the signal. The detection limit (DL) acquired by this developed method was 0.22 μg/L (194.1 nm), which was nearly 82 times lower than that obtained by pneumatic nebulization (PN). The relative standard deviation (RSD) was 1.4% ($n = 14$) for a 50 μg/L standard. Blank solution (HNO_3, pH 1) can effectively elute mercury residue. Its accuracy and practicality were also demonstrated by the determination of GBW10029 (fish) certified reference material, shrimp, crawfish, soil and human hair samples. The results showed good consistency with the certified values and the values obtained using inductively coupled plasma–mass spectrometry.

The accurate determination of mercury has aroused widespread interest due to its ultra-high toxicity to human organs, such as lungs, even at an extremely low concentration level [1,2]. Hence, trace and ultra-trace analysis of mercury is in great demand, and the samples are frequently accompanied by a relatively complicated matrix. This brings great challenges to some analytical techniques now available, such as inductively coupled plasma-optical emission spectrometry (ICP-OES), which is extensively used for its high stability, multi-element simultaneous analysis and convenient operations. Pneumatic nebulizer is commonly adopted to introduce liquid samples in this technology. However, the sensitivity of some elements (*e.g.*, Hg) is not satisfying due to the low transport efficiency [3]. Consequently, alternative sample introduction techniques are being developed to perform online separation and/or preconcentration prior to measurement [4–6].

Chemical vapor generation (CVG) is an important sample introduction technique, which brings about effective separation of matrix, high transport efficiency and selectivity [7,8]. Traditional CVG technologies are mainly based on chemical reducing agents, such as tetrahydroborate acid (THB-acid) system for hydride generation (HG). With mature instrument and high vapor generation efficiency, HG is considered to be the most extensively used and successful method at present [9,10]. The aforementioned tetrahydroborate ($NaBH_4/KBH_4$), however, is expensive and unstable, and needs to be prepared afresh. Photochemical vapor generation (PVG) technology avoids the use of expensive chemical reagents ($NaBH_4/KBH_4$) and merely requires low-molecular weight organic compounds (LMWOCs) doped in the sample [11,12]. The addition of LMWOCs is an essential step in the PVG process, and photocatalyst or metal sensitizer are usually added to the sample to optimize the efficiency, which means that the method usually needs a relatively complex reaction medium [13–15].

Recently, considerable attention has been paid to technologies of vapor generation induced by microplasma, including dielectric barrier discharge (DBD) [16–23], alternating current driven solution electrode glow discharge (ac-SEGD) [24,25], solution anode glow discharge (SAGD) [26,27], electrolyte-as-cathode glow discharge (ELCAD) [28], and its derivative techniques, *e.g.*, solution cathode glow discharge (SCGD) [29–33], hanging drop cathode-atmospheric pressure glow discharge (HDC-APGD) [34]. Although the mechanism of plasma induced vapor generation (PIVG) remains to be clarified, it is believed that the plasma is rich in solvated electrons, excited states, ions, free radicals (*e.g.*, $^{\bullet}H$, $^{\bullet}OH$) and other reactive substances (*e.g.*, H_2, H_2O_2), which are related to reduction reactions and directly induce the almost instantaneous gener-

* Corresponding author.
E-mail address: wangzheng@mail.sic.ac.cn (Z. Wang).

https://doi.org/10.1016/j.cclet.2021.09.107
1001-8417/

ation of volatile species during sample introduction [10,22,35-37]. Therefore, PIVG technique is considered to be an excellent alternative sampling technique with the advantages of fast analysis speed, small matrix effect and simple reaction medium.

In PIVG technologies, ELCAD was first chosen to serve as a sampling unit [28], and its spin-off technologies have also been preliminarily proved to have the potential to generate vapors of various elements (*e.g.*, Ag, Bi), especially Hg [29,31–34]. In 2008, Zhu *et al.* [33] used SCGD as a new sample introduction method for ICP-OES to overcome the weakness of low sensitivity of ICP-OES in the determination of mercury. The analysis signal was approximately 16 times higher than that obtained with conventional pneumatic nebulization (PN). Furthermore, the intensity of the Hg emission was even higher by a factor of 2–3 in the presence of LMWOCs added to the sample solution. Subsequently, the same arrangement was also successfully applied to generation of the volatile species of Os [29] and I [31]. Very recently, Swiderski *et al.* [34] reported the use of HDC-APGD as a new method of sample introduction for ICP-OES with a low sample uptake (0.56 mL/min) and entire sample consumption. The developed arrangement resulted in higher intensities of emission lines of studied elements (2 times higher on average) than those obtained with PN.

It is universally known that a certain amount of water, whether in the form of aerosol droplets or water vapor, will affect the temperature and electron number density of ICP, thus affecting the stability and strength of the signal [38,39]. And the moisture contained in carrier gas will cause the dilution of the mercury vapor and additional consumption of energy of ICP [40]. However, the water vapor produced by SCGD is cooled and aggregated into droplets during transportation or gets into a subsequent detector with relatively high content [33,34]. Therefore, the performance of the hyphenated technique can be improved by further reducing the water load.

Thus, we herein presented a new sample introduction for ICP-OES based on SCGD-induced vapor generation technology. A gas-liquid separator (GLS), a dryer and a spray chamber were used to remove as much water as possible, further improving the robustness of ICP. Experimental parameters thereof, *e.g.*, acid type, discharge voltage, solution flow rate, discharge gap, carrier gas flow rate and ICP power were thoroughly optimized. Besides, analytical figure of merit was determined. The detection limit (DL) of this method was compared with that obtained by PN and the results of similar works.

The design of SCGD closure is shown in Fig. S1 (Supporting information). The SCGD used a tapered tungsten rod (ø = 2.6 mm) as the anode and right below the tungsten rod was a glass capillary (ø in/out = 0.38/1.1 mm). The solution overflowed from the tip of the capillary to conduct with a grounded graphite rod (ø = 5 mm). The graphite rod had a hole drilled for vertical insertion of the capillary. A peristaltic pump (BT100–1 L, Lange Constant Flow Pump, Baoding, China) transported the sample solution in the glass capillary and the waste. The distance between the tip of the tungsten rod and the surface of the sample solution was fixed at approximately 3 mm. The SCGD closure avoided the existence of waste reservoir for conduction, consequently improving its portability and assemblability. The gas inlet was continuously filled with flowing argon gas, which delivered the substances including atoms, ions and free radicals produced by the microplasma. High voltage power supply (HSPY-600, Hansheng Puyuan, Beijing, China) provided around 1000 V applied between the two electrodes, and a ballast resistor (1.2 kΩ, 150 W) was inserted in the circuit to prevent the conversion of glow discharge to arc discharge. The knotted part of the injection pipeline refrained from the potential discontinuity of the introduction. In this work, by squeezing the elastic air chamber, the solution height was the highest in an instant, so as to realize rapid ignition.

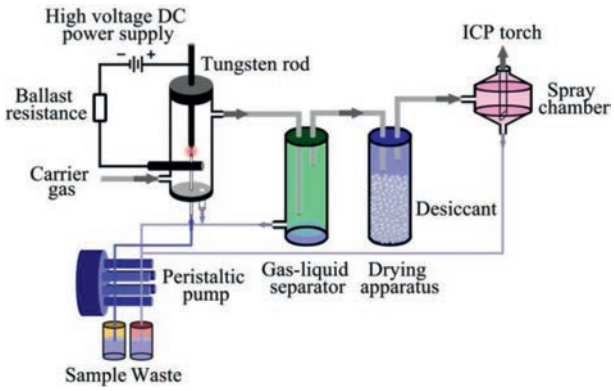

Fig. 1. Schematic diagram of the SCGD-ICP-OES system.

The products from SCGD containing mercury vapor, was successively transported to the GLS, dryer, cyclonic spray chamber, and ultimately reached the torch of ICP-OES (Agilent 725, Agilent Technology, Shanghai, China). The discharge gas, *i.e.*, carrier gas, flowed in the pipe of nebulizer gas. Its flow rate was directly controlled by the operating system of the ICP spectrometer, so no additional gas flowmeter was required. GLS was simply composed of a sealed container and the dryer had a similar structure with some desiccant in it. Calcium chloride was used as a desiccant in this work. The employment of GLS and dryer greatly ameliorated the obstruction of gas pipe and ICP instability caused by water vapor condensation in the gas path. On the other hand, mercury vapor was enriched while water vapor was removed. GLS and dryer here also acted as gas buffers. A scheme of the SCGD-ICP-OES experimental setup is given in Fig. 1.

The emission line of Hg at 194.1 nm was selected in parameter optimization experiment, anti-interference test, stability test and memory effect evaluation due to its lowest DLs. Followingly, the DLs of the other two sensitive lines (184.8 nm and 253.6 nm) under the optimal conditions were calculated for comparison with the results in the literature. The operating conditions of the ICP-OES instrument with PN are shown in Table S1 (Supporting information). For SCGD-ICP-OES, the added optimization of radio frequency (RF) power and nebulizing Ar (carrier gas) flow rate will be discussed in detail later. All measurements were made in eleven replicates ($n = 11$), and average values were taken into consideration.

The detailed experimental reagents as well as sample treatment are given in Text S1 (Supporting information).

In the proposed method, SCGD acted as the sampling system, and its operating conditions (acid type, discharge voltage, solution flow rate, discharge gap), which are related to evaporation efficiency, were optimized here to obtain the best analytical performance.

Acid with pH 1 is a common electrolyte solution. One fact to note is that different acid matrices will introduce different anions at a high concentration (0.1 mol/L) into the sample, which has a certain impact on the analysis results. Therefore, the effect of different acids (HNO_3, H_2SO_4, HCl, pH 1) on the analytical performance of the method was studied. It can be seen from the optimization results in Fig. S2a (Supporting information) that when H_2SO_4 and HCl were used, the signal and DLs of mercury were significantly worse than those using HNO_3. The ionic radii of Cl^-, NO_3^- and SO_4^{2-} are 181, 165 and 244 pm, respectively [41]. The relatively large anion size of H_2SO_4 leads to the lower mobility (conductivity), current and power of the electrolyte, resulting in the lower vapor generation efficiency [42,43]. The lowest signal intensity of Hg with HCl as the substrate is mainly due to the forma-

tion of strong complex with Hg^{2+}, which caused severe signal suppression. In addition, considering that HNO_3 is a promising aqueous sample digestion reagent with good chemical compatibility, it was selected.

The voltage applied affects the stability and energy of discharge, and the result of optimization is shown in Fig. S2b (Supporting information). With the increase of voltage, the energy and power of microplasma enhanced, and higher mercury vapor generation efficiency was obtained [44]. However, when the voltage was great enough, red heat effect occurred. Even if stronger signal intensity was obtained in higher voltage, the DLs were not significantly improved due to the larger background fluctuation. And long-term stable discharge could not be maintained, which was not conducive to the practical application. Similar results have been reported in many literature [41,45,46]. Furthermore, long time high voltage supply will accelerate the loss of anode rod and the formation of oxide layer on its surface. For the above reasons, the discharge voltage was set to 1030 V.

Fig. S2c (Supporting information) reveals the relevance between sample flow rate and signal intensity of Hg. Considering the ease and stability of ignition, sample flow rate varied from 2.7 mL/min to 3.9 mL/min. The DL reduced when the sample flow rate increased from 2.7 mL/min to 3.3 mL/min. This may be a consequence of the rise of the solution surface height. The exposed surface area of sample expanded and more analytes entered the microplasma. In addition, the increased conductivity is also one of the important factors of signal enhancement. However, it was found that too high solution flow rate resulted in poor signal strength. The increase of the flow rate would shorten the residence time of the analytes in the microplasma, making analytes out with the waste before entering the plasma from the solution. Additionally, the generated water vapor and its products may combine with the analyte atoms, reducing the energy of the excited atoms or the number of electrons in the microplasma. This moisture also had an adverse effect on the ICP torch behind. Therefore, a sample flow rate of 3.3 mL/min, was selected for all subsequent experiments.

Fig. S2d (Supporting information) shows the effect of discharge gap. Too short, arc discharge occurs. Too long, it is difficult to ignite. It was observed that larger discharge gap brought about higher signal intensity. The SCGD cell with a discharge gap of 2 mm has a serious red heat phenomenon, while the ignition of SCGD cell with a discharge gap of 4 mm was difficult and the microplasma was easily affected by the airflow, which was not conducive to the subsequent optimization of carrier gas flow rate. Considering the easiness of ignition and the similar DLs with 3 and 4 mm, the discharge gap of 3 mm was finally adopted.

As the detector of the system, the influential parameters of ICP-OES (nebulizing/carrier gas flow rate, RF power) were also optimized carefully.

Argon played the role of transporting aerosol containing mercury atoms. The effect of carrier gas (Ar) flow rate on the DL values was evaluated between 250 mL/min and 650 mL/min, as described in Fig. S3a (Supporting information). At the beginning, with the increase of carrier gas flow rate, the transport efficiency raised gradually, resulting in decreased DL values. When it reached 450 mL/min, the larger the carrier gas flow rate was, the higher the detection limit would be due to the dilution and cooling effect of carrier gas. Therefore, the carrier flow rate of 450 mL/min was recognized as the most beneficial for Hg and considered as optimal value for further work.

It is well known that almost all spectral line intensities increase with increasing power. However, excessive power will also lead to enhanced background radiation and deteriorated signal-to-background ratio (SBR). The above statement makes the explanation about the results of the newly proposed system (Fig. S3b in Supporting information). With the increase of power, the signal increased due to increase of the excitation ability, which is consistent with the literature published previously [29]. However, it is worth noting that the improvement of excitation ability would also have an effect on the background, so the DL was not significantly improved, showing a slight downward trend, especially after 1.3 kW. Therefore, considering energy consumption, the power of 1.35 kW was selected as the optimization condition for the remaining parts of the study.

Table 1
Effect of foreign ions on the Hg (194.1 nm) emission line intensity (expressed as percent recovery) determined by SCGD-ICP-OES.

Concomitant	Concentration (mg/L)	Recovery (%)
Fe^{3+}	5	101 ± 1.7
Mn^{2+}	5	100 ± 1.4
Ni^{2+}	5	93 ± 1.0
Co^{2+},	5	90 ± 0.9
Pb^{2+}	5	97 ± 0.7
Cd^{2+}	5	98 ± 2.1
Mg^{2+}	5 (50)	103 ± 1.4 (106)
Ca^{2+}	5 (50)	105 ± 1.3 (101)
K^{+}	5 (50)	103 ± 0.9 (98)
Na^{+}	5 (50)	106 ± 0.9 (101)
SO_4^{2-}	5 (50)	100 ± 1.1 (101)
MnO_4^{-}	5 (50)	94 ± 2.2 (65)
$Cr_2O_7^{2-}$	5 (50)	100 ± 1.0 (92)
Cl^{-}	0.1 mol/L	18 ± 0.3
Cl^{-}	0.01 mol/L	40 ± 0.8
Cl^{-}	0.001 mol/L	72 ± 1.5

Note: values in brackets indicate higher test contamination concentrations and corresponding recoveries.

As shown in Table 1, to evaluate the suitability of the proposed methods for real samples analysis, the robustness of SCGD-ICP-OES to matrix induced interference was tested. The recoveries of Hg^{2+} were determined in the presence of transition, alkali and alkaline earth metals and anions. These potential interfering ions were added with the concentration of 5 mg/L to the single element standard solution at the concentration of 50 μg/L. The higher concentration (50 mg/L) of Mg^{2+}, Ca^{2+}, K^{+} and Na^{+} was dictated by the fact that these elements are usually found in samples in more abundant quantities. The recoveries obtained were between 90% and 110% for all metal interfering ions, sulfate and dichromate at the tested concentrations. For MnO_4^{-}, although the response decreased to 65% at 50 mg/L, the interference could be negligible at 5 mg/L. Unfortunately, similar to other PIVG technologies [23,33], chloride ions could suppress the mercury response to some extent, mainly due to the strong complexation between mercury and chloride ions. Therefore, samples treated/digested with hydrochloric acid or perchloric acid are not suitable for direct determination by this method.

The performance of SCGD-ICP-OES method was evaluated under the optimal experimental parameters: HNO_3 as electrolyte, discharge voltage of 1030 V, solution flow rate of 3.3 mL/min, discharge gap of 3 mm, carrier gas flow rate of 450 mL/min, and ICP power of 1.35 kW. As shown in Fig. S4 (Supporting information), the calibration curve was linear within the Hg concentration range of 2−500 μg/L, with excellent linear correlation coefficient being calculated ($R^2 \geq 0.999$). The DL was 0.22 μg/L (194.1 nm) under the full set of optimization parameters ($DL = n \times SD/k$. Where n is the confidence coefficient and 3 is generally chosen as the experimental value, SD was standard deviation of the blank solution, k was the slope of the calibration curve). The stability of experimental detection is represented by RSD, which is shown in Fig. 2. The signal intensities with and without a dryer were also compared. In the study, the RSD value for 50 μg/L Hg solution measured every two minutes with a dryer was 1.4%, which was better than value obtained without a dryer. The corresponding signal was also increased to 1.2 times after adding a dryer.

Table 2
Comparison of DLs for Hg^{2+} in different analytical methods.

Method	Detection limit (μg/L)			
	184.8 nm	194.1 nm	253.6 nm	Ref.
PN-ICP-OES	64	18	22	Agilent 725
SCGD-ICP-OES	0.31	0.22	0.25	Present work
SCGD-ICP-OES[a]	—	—	0.7	[33]
SCGD-OES	—	—	20	[47]
HG-ICP-OES	0.21	0.21	0.55	[48]
PVG-ICP-OES	—	—	0.1	[49]
DBD-ICP-OES[a]	0.09	—	—	[20]
SD-SEGD-CVG-AFS[b]	—	—	0.01	[25]
PVG-SCGD-OESTF-DBD-DBD-OES[a]	—	—	0.2,0.2	[23,50]

— Not studied.
[a] Sensitization of formic acid.
[b] Couple to multiwall carbon nanotubes assisted matrix solid-phase dispersion (MWCNTs-MSPD).

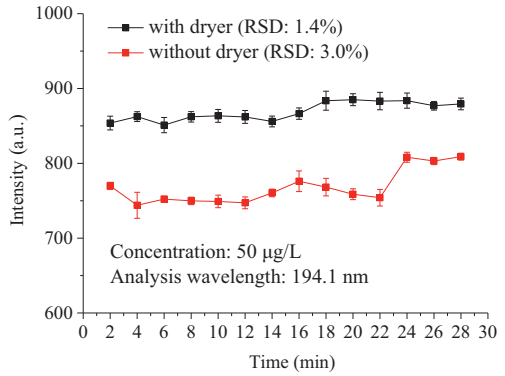

Fig. 2. Comparison of the stability of the emission signals of mercury standard solution before and after adding dryer.

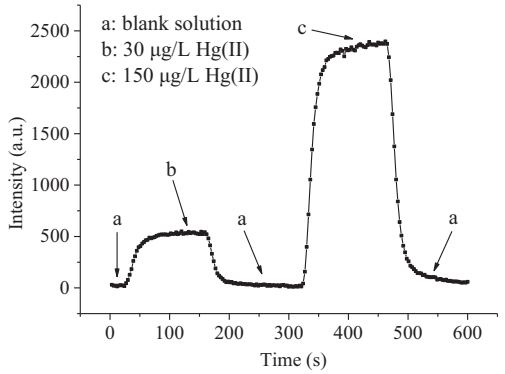

Fig. 3. Memory effect of Hg. The graph shows the Hg signal intensity as a function of running time (s).

Mercury absorption in tubings, spray chambers and nebulizers accumulating in the ICP sample introduction system is a commonly known problem. Mercury standard solutions of 30 and 150 μg/L were sampled for 2 min continuously, and then washed with blank. The signal profile is illustrated in Fig. 3 and no significant memory effect was observed using the proposed system. The residual signals of two concentrations of mercury standard solution dropped to the background level during the washout for about 45 s and 90 s, respectively.

The DLs of SCGD-ICP-OES and PN-ICP-OES were shown in Table 2, compared with the results reported in the literature (mainly other vapor generation devices coupled with ICP-OES). The DL of 0.22 μg/L (194.1 nm) was reduced by nearly two orders of magnitude by replacing pneumatic nebulization with SCGD for mercury vapor generation, manifesting high sensitivity. Compared with the SCGD-CVG firstly reported [33], the DL obtained by this method was improved. The sampling system is distinct in the design of vapor transportation path. The combination of GLS, dryer and spray chamber can remove moisture as much as possible, greatly enhancing the stability of signal intensity. For another, more parameters directly related to signal sensitivity, such as ICP power and microplasma discharge gap, are also discussed here. Although not as good as DBD-ICP-OES [20] or single drop (SD)-SEGD-CVG-atomic fluorescence spectrometry (AFS) [25], the organic small molecule and solid phase extraction technology were not used here for sensitization. Thin film(TF)-DBD-DBD-OES is the application of PIVG technology in micro spectrometer, which possesses the advantage of portability and compactness [23]. However, the detection limit is one order of magnitude higher than that of this work before using formic acid. The remaining results show the superiority of SCGD-ICP-OES over stand-alone SCGD-OES [47] and the comparability with other traditional CVG-ICP-OES technologies (HG [48] or PVG [49,50]), indicating the ability of SCGD as a simple, efficient and green alternative sampling technology.

To verify the accuracy of the developed SCGD-ICP-OES system, it was applied in the analysis of GBW10029 CRMs, shrimp, crawfish, human hair and soil samples. Considering the complex matrix in the soil, the standard addition method was adopted. The obtained results (Table 3) showed a good agreement with the certified reference values and the results obtained by inductively coupled plasma-mass spectrometry (ICP-MS). A series of recovery tests were carried out by spiking 3 μg/kg, 3 μg/kg, 3.5 μg/kg and 10 μg/kg standard solution with the shrimp, crawfish, human hair-2 and soil samples respectively for the endogenous concentrations (after dilution) were below the quantization limit (QL, $QL = 10 \times SD/k$) of the proposed method. The results show that the two methods were consistent in both bottom values and spiked values.

In Summary, a solution cathode glow discharge-vapor generator, accompanied by a gas-liquid separator and a dryer, was used as the sample introduction system of ICP-OES for ultra-high sensitive analysis of mercury. The results showed that SCGD had excellent vapor generation efficiency for Hg, which was comparable with other chemical vapor generation technologies like HG and PVG. Appliance of GLS and dryer enhanced the stability and sensitivity of the combined instrument. Under the optimal conditions, the DL reached 0.22 μg/L (194.1 nm) in the absence of small molecular organics. Compared with the DL obtained by traditional pneumatic nebulization, the modified SCGD-ICP-OES system offered 82-fold lower detection limit. In spite of good performance obtained by this method, the mechanism of SCGD-vapor generation for sensitization is still undefined, and more efforts are needed to explore it in the future work. In addition, the premium vapor generation ef-

Table 3
Determination of Hg concentration in certified reference material, shrimp, crawfish, soil and human hair samples. Mean ± SD (n = 3).

Sample	SCGD-ICP-OES (μg/kg)	ICP-MS (μg/kg)	Mercury added, detected by SCGD-ICP-OES (μg/kg)*	Recovery (%)
GBW10029(fish)	781 ± 17	839 ± 37	–	–
Shrimp	nd	nd	3.13 ± 0.06	104
Crawfish	nd	16 ± 1	2.86 ± 0.59	95
Human hair-1	340 ± 21	359 ± 17	–	–
Human hair-2	nd	33 ± 1	3.23 ± 0.22	92
Human hair-3	236 ± 20	231 ± 27	–	–
Soil	nd	nd	9.49 ± 0.48	95

nd, not detectable.
* found in the test solutions (dilution ratio was 500 for soil and 100 for others).

ficiencies of SCGD for other elements deserve to be studied, which will help to retain the superiority of multi-element simultaneous analysis of ICP-OES.

Declaration of competing interest

The authors declare that they have no known competing financial interests or personal relationships that could have appeared to influence the work reported in this paper.

Acknowledgments

This work was supported by the Instrument Development Project of the Chinese Academy of Sciences (No. YZ201539), the National Natural Science Foundation of China (No. 21175145), and the Shanghai Technical Platform for Testing and Characterization on Inorganic Materials (No. 19DZ2290700).

Supplementary materials

Supplementary material associated with this article can be found, in the online version, at doi:10.1016/j.cclet.2021.09.107.

References

[1] K.M. Rice, E.M. Walker Jr., M. Wu, C. Gillette, E.R. Blough, J. Prev. Med. Public. Health. 47 (2014) 74–83.
[2] Y.Z. Li, Q.Q. Zhou, B. Ren, et al., Trends and Health Risks of Dissolved Heavy Metal Pollution in Global River and Lake Water from 1970 to 2017, in: P. De-Voogt (Ed.), Reviews of Environmental Contamination and Toxicology, 251, Springer Nature Switzerland, Basel, 2020, pp. 1–24.
[3] J. Borkowska-Burnecka, A. Lesniewicz, W. Zymicki, Spectrochim. Acta Part B 61 (2006) 579–587.
[4] M.M.L. Guerrero, E.V. Alonso, J.M.C. Pavon, M.T.S. Cordero, A.G. de Torres, J. Anal. At. Spectrom. 31 (2016) 975–984.
[5] M. Garcia, M. Angel Aguirre, A. Canals, Anal. Bioanal. Chem. 409 (2017) 5481–5490.
[6] J.C. Garcia-Mesa, P.M. Leal, M.M.L. Guerrero, E.I.V. Alonso, Microchem. J. 150 (2019) 104141.
[7] M. Yuan, X. Peng, F. Ge, et al., Chin. Chem. Lett. 31 (2020) 2814–2818.
[8] P. Pohl, P. Jamroz, M. Welna, A. Szymczycha-Madeja, K. Greda, TrAC Trends Anal. Chem. 59 (2014) 144–155.
[9] T. Chen, Y. Lin, H. Li, et al., Chin. Chem. Lett. 31 (2020) 2678–2682.
[10] X. Liu, Z.L. Zhu, P.J. Xing, H.T. Zheng, S.H. Hu, Spectrochim. Acta Part B 167 (2020) 105822.
[11] Y.H. He, X.D. Hou, C.B. Zheng, R.E. Sturgeon, Anal. Bioanal. Chem. 388 (2007) 769–774.
[12] R.E. Sturgeon, P. Grinberg, J. Anal. At. Spectrom. 27 (2012) 222–231.
[13] Z.R. Zou, J. Hu, F.J. Xu, X.D. Hou, X.M. Jiang, TrAC Trends Anal. Chem. 114 (2019) 242–250.
[14] Y.L. Wang, L.L. Lin, J.X. Liu, et al., Analyst 141 (2016) 1530–1536.
[15] R.E. Sturgeon, Anal. Chem. 87 (2015) 3072–3079.
[16] Z.F. Liu, Z. Xing, Z.Y. Li, et al., J. Anal. At. Spectrom. 32 (2017) 678–685.
[17] Y.X. Li, Z.L. Zhu, H.T. Zheng, L.L. Jin, S.H. Hu, J. Anal. At. Spectrom. 31 (2016) 383–389.
[18] Q. Wu, Z. Zhu, Z. Liu, et al., J. Anal. At. Spectrom. 27 (2012) 496–500.
[19] Z.F. Liu, Z.L. Zhu, Q.J. Wu, S.H. Hu, H.T. Zheng, Analyst 136 (2011) 4539–4544.
[20] X. Wu, W.L. Yang, M.G. Liu, X.D. Hou, C.B. Zheng, J. Anal. At. Spectrom. 26 (2011) 1204–1209.
[21] P. Pohl, K. Greda, A. Dzimitrowicz, et al., TrAC Trends Anal. Chem. 113 (2019) 234–245.
[22] Q. He, Z.L. Zhu, S.H. Hu, Rev. Anal. Chem. 33 (2014) 111–121.
[23] A.Q. Leng, Y.F. Tian, M.X. Wang, et al., Zheng, Chin. Chem. Lett. 28 (2017) 189–196.
[24] Z.A. Li, Q. Tan, X. Hou, K. Xu, C. Zheng, Anal. Chem. 86 (2014) 12093–12099.
[25] Q. Chen, Y. Lin, Y.F. Tian, et al., Anal. Chem. 89 (2017) 2093–2100.
[26] X. Liu, Z.F. Liu, Z.L. Zhu, et al., Anal. Chem. 89 (2017) 3739–3746.
[27] K. Greda, M. Gorska, M. Welna, P. Jamroz, P. Pohl, Talanta 199 (2019) 107–115.
[28] T. Cserfalvi, P. Mezei, J. Anal. At. Spectrom. 20 (2005) 939–944.
[29] Z.L. Zhu, C.Y. Huang, Q. He, et al., Talanta 106 (2013) 133–136.
[30] P.C. Zheng, H.D. Liu, J.M. Wang, et al., J. Anal. At. Spectrom. 30 (2015) 867–874.
[31] Z.L. Zhu, Q. He, Q. Shuai, H.T. Zheng, S. Hu, J. Anal. At. Spectrom. 25 (2010) 1390–1394.
[32] Q. He, Z.L. Zhu, S.H. Hu, L.L. Jin, J. Chromatogr. A 1218 (2011) 4462–4467.
[33] Z.L. Zhu, G.C.Y. Chan, S.J. Ray, X. Zhang, G.M. Hieftje, Anal. Chem. 80 (2008) 7043–7050.
[34] K. Swiderski, M. Welna, K. Greda, P. Pohl, P. Jamroz, Anal. Bioanal. Chem. 412 (2020) 4211–4219.
[35] S. Samukawa, M. Hori, S. Rauf, et al., J. Phys. D-Appl. Phys. 45 (2012) 253001.
[36] P. Rumbach, M. Witzke, R.M. Sankaran, D.B. Go, J. Am. Chem. Soc. 135 (2013) 16264–16267.
[37] R.K. Marcus, B.T. Manard, C.D. Quarles, J. Anal. At. Spectrom. 32 (2017) 704–716.
[38] I. Novotny, J.C. Farinas, J.L. Wan, E. Poussel, J.M. Mermet, Spectrochim. Acta Part B 51 (1996) 1517–1526.
[39] J.W. Olesik, J.A. Hartshorne, N. Casey, E. Linard, J.R. Dettman, Spectrochim. Acta Part B 176 (2021) 106038.
[40] S.E. Long, R.D. Snook, R.F. Browner, Spectrochim. Acta Part B 40 (1985) 553–568.
[41] J. Yu, S.X. Yang, D.X. Sun, et al., Microchem. J. 128 (2016) 325–330.
[42] R.M. Huang, Z.L. Zhu, H.T. Zheng, et al., J. Anal. At. Spectrom. 26 (2011) 1178–1182.
[43] P. Mezei, T. Cserfalvi, H.J. Kim, M.A. Mottaleb, Analyst 126 (2001) 712–714.
[44] R.K. Marcus, W.C. Davis, Anal. Chem. 73 (2001) 2903–2910.
[45] M.A. Mottaleb, Y.A. Woo, H.J. Kim, Microchem. J. 69 (2001) 219–230.
[46] P.C. Zheng, Y.J. Luo, J.M. Wang, et al., J. Anal. At. Spectrom. 36 (2021) 1228–1234.
[47] X.X. Peng, X.H. Guo, F. Ge, Z. Wang, J. Anal. At. Spectrom. 34 (2019) 394–400.
[48] M. Grotti, C. Lagomarsino, R. Frache, J. Anal. At. Spectrom. 20 (2005) 1365–1373.
[49] C.B. Zheng, R.E. Sturgeon, C. Brophy, X.D. Hou, Anal. Chem. 82 (2010) 3086–3093.
[50] J.M. Mo, Q. Li, X.H. Guo, G.X. Zhang, Z. Wang, Anal. Chem. 89 (2017) 10353–10360.